MCB Accepts, published online ahead of print on 26 November 2012
Mol. Cell. Biol. doi:10.1128/MCB.01020-12

Cell-cycle-dependent transcriptional and translational DNA-damage response of ribonucleotide reductase genes in *S. cerevisiae*

Aprotim Mazumder[a], Katja Tummler[a], Mark Bathe[a,#], Leona D. Samson[a,b,#]

[a] Department of Biological Engineering and Center for Environmental Health Sciences, [b] Department of Biology, Massachusetts Institute of Technology, Cambridge, MA 02139, USA

[#] To whom correspondence should be addressed: lsamson@mit.edu; mark.bathe@mit.edu

Running-title: Cell-cycle-dependent DNA-damage response of yeast RNR

Number of figures: 6

Number of words in the Abstract: 199

Number of words in the Main-text (excluding Abstract, Materials and Methods, References and Figure Legends): 2720

Number of words in the Materials and Methods section: 1091

Number of references: 41

Number of Supplementary figures: 11

ABSTRACT

The ribonucleotide reductase (RNR) enzyme catalyzes an essential step in the production of deoxyribonucleotide triphosphates (dNTPs) in cells. Bulk biochemical measurements in synchronized *S. cerevisiae* cells suggest that *RNR* mRNA production is maximal in late G1 and S-phase; however, damaged DNA induces *RNR* transcription throughout the cell cycle. But such en masse measurements reveal neither cell-to-cell heterogeneity in responses, nor direct correlations between transcript and protein expression or localization in single cells which may be central to function. We overcame these limitations by simultaneous detection of single *RNR* transcripts and also Rnr proteins in the same individual asynchronous *S. cerevisiae* cells, with and without DNA-damage by methyl methanesulfonate (MMS). Surprisingly, RNR subunit mRNA levels were comparably low in both damaged and undamaged G1 cells, and highly induced in damaged S/G2 cells. Transcript numbers became correlated with both protein level and localization only upon DNA-damage in a cell-cycle dependent manner. Further we showed that the differential *RNR* response to DNA-damage correlated with variable Mec1 kinase activity in the cell-cycle in single cells. The transcription of *RNR* genes was found to be noisy and non-Poissonian in nature. Our results provide vital insight into cell-cycle-dependent RNR regulation under conditions of genotoxic stress.

INTRODUCTION

Unrepaired DNA-damage can result in cell growth arrest, apoptosis, premature aging, neurodegeneration and cancer (16, 18). Because most DNA repair pathways require de novo synthesis of DNA, damaged DNA signals the increased production and activation of the RNR enzyme (25, 36, 40). In almost all eukaryotes the functional RNR enzyme consists of a large and a small subunit (25). The *S. cerevisiae* genes *RNR1* and *RNR3* code for the large subunit proteins, while *RNR2* and *RNR4* code for of the small subunit proteins (Figure 1). The active form of the small subunit is a Rnr2-Rnr4 heterodimer (9, 26), and it relocalizes to the cytoplasm from the nucleus upon DNA damage (2, 36) to make the functional holoenzyme with the large subunit. Additionally, upon DNA damage the transcription of all *RNR* genes are induced by the Mec1-Rad53 pathway (20, 35), which also controls the subcellular localization of the Rnr2-Rnr4 heterodimer (23) and the activation of the RNR enzyme (39, 41). Much of our understanding of the response of RNR to DNA damage as a function of cell-cycle stage comes from bulk

biochemical studies involving the model eukaryote *S. cerevisiae* (Figure 1) (14, 15, 19). However, the synchronization methods employed in these studies may alter normal cell behavior. Further, mean-values probed in bulk population studies mask information on cell-to-cell variability in response, which is clearly resolvable with single-cell level imaging (1, 6, 29, 32). Moreover, mRNA and protein levels and localization are usually measured in separate experiments, and few studies have explored the measurement of both gene products in the same cells.

As a consequence, it remains unclear whether *RNR* genes are induced uniformly across cells by DNA damage via a homogeneous amplification of the normal cell-cycle transcript distributions, or whether cell-cycle-stage-specific amplification of transcripts occurs. Additionally, correlated variation in protein and mRNA levels in individual cells in distinct stages of the cell cycle with and without genotoxic stress remains unexplored. For example, mRNA and protein levels were recently found to become correlated for a number of genes under conditions of osmotic stress using bulk mass spectrometry (22), whereas little-to-no correlation between mRNA and protein has been observed in several bulk and single-cell studies in unperturbed cells (12, 17, 32). This discrepancy is likely to be because of the longer half-lives of most proteins that results in slower fluctuations in their numbers with respect to mRNAs that typically degrade rapidly in a programmed manner (5, 32, 34).

To overcome these limitations and reveal the possible cell-cycle-dependence of Rnr mRNA and protein to DNA damage, we assayed the transcriptional response of the RNR subunit genes by imaging single transcripts with fluorescence in situ hybridization (FISH) (28, 31, 37, 38), and subsequently combined this technique with immunofluorescence detection of Rnr proteins to simultaneously investigate their translational responses in the same individual cells as a function of the cell-cycle.

MATERIALS AND METHODS

Cell growth and mRNA FISH. All chemicals were from Sigma-Aldrich (St. Louis, MO), Invitrogen (Carlsbad, CA) or Ambion (Applied Biosystems, Austin, TX), unless otherwise noted. BY4741 cells were typically grown in YPD medium at 30°C with shaking. For experiments with RC634 cells YPDA (YPD with 0.003% Adenine hemisulfate) medium was used to avoid fluorescent purine precursors accumulating in the vacuoles. FISH was performed following

earlier studies in yeast (28, 31, 37, 38). Cells were diluted to an optical density (at 600 nm, OD_{600}) of 0.15 in the appropriate medium from an overnight saturated culture, and allowed to grow to an OD_{600} of 0.5 in a 10 ml volume for each experiment. At this point the culture was divided into two halves and cells were diluted in an equal volume of either control or MMS containing medium and allowed to grow for another hour. At this time point both broad cell-cycle categories are still represented in the population. The final MMS concentration was 0.02% like in previous works (36). For FISH experiments, cells were fixed for 45 minutes by direct addition of formaldehyde to a final concentration of 4%. Cells were then washed twice in Buffer B (1.2 M sorbitol, 100 mM potassium phosphate in nuclease-free water), spheroplasted in Buffer B with 100 mU/µl Lyticase, 0.06 mg/ml phenylmethylsulfonyl fluoride (PMSF), 28 mM β-Mercaptoethanol, 10 mM Vanadyl Ribonucleoside Complex (VRC, New England Biolabs (Ipswich, MA)) at 30°C, and washed twice again in Buffer B. The cells were then resuspended in 70% Ethanol and left overnight at 4°C. The cells were then resuspended for 5 minutes in wash buffer (2X SSC, 25% Formamide in nuclease free water) and resuspended in hybridization buffer (10 mM VRC, 1mg/ml BSA, 20X SSC, 0.5 mg/ml *E.coli* tRNA, 0.5mg/ml ssDNA, 100mg/ml Dextran sulfate, 25% Formamide, 2X SSC, in nuclease-free water) with Alexa-568 labeled probes against the target mRNA. mRNA probes were obtained from Biosearch Technologies (Novato, CA). Hybridization was allowed proceed overnight at 30°C. The cells were then washed with wash buffer and stained for 30 minutes with 1µg/ml DAPI to stain the DNA. The cells were then washed and resuspended in 2X SSC and mounted in ProLong Gold Antifade reagent on cover-slides.

mRNA probe design. Each *RNR* gene was targeted by 40 of 20-nucleotide long DNA oligo probes each with a 3' Alexa 568 fluorophore. When designing probes we used bioinformatics to eliminate any probe which can potential cross-hybridize between genes like *RNR1* and *RNR3* which show large similarities (13) in nucleotide sequence (Supplementary Figure S1). The efficacy of this approach is apparent in the fact that control untreated asynchronous cells expectedly do not show any *RNR3* expression, while a subpopulation of the same cells clearly stain for high numbers of *RNR1* in keeping with the known large fluctuations of *RNR1* expression in course of the normal cell cycle (15) (Figure 2B; Supplementary Figure S7). This indicates that *RNR3* probes do not cross-hybridize with the ubiquitous *RNR1* mRNA.

Simultaneous detection of mRNA and protein. mRNA FISH was performed as before, followed by immunofluorescence for proteins. All reagents were specifically made from nuclease-free materials, to avoid degradation of transcripts. We verified that largely same mRNA numbers were obtained when FISH was performed alone and when FISH was

performed with immunofluorescence (Supplementary Figure S2). Following mRNA FISH, subsequent steps were performed in the blocking solution made from nuclease-free materials. Cells were blocked in 1% BSA in PBS for 1 hour. Cells were stained with the primary antibodies at 1:1000 dilution for 3 hours, and then with the Alex-647-tagged secondary antibodies at 1:200 dilution for 1.5 hours following an earlier work (36). Cells were washed in 2X SSC and mounted in ProLong Gold Antifade reagent on cover-slides. The H2A-S129p antibody was obtained from Upstate (Millipore, Billerica, MA). All the Rnr antibodies used have been used in a previous study that demonstrated the translocation of Rnr2 and Rnr4 from the nucleus to the cytoplasm upon DNA damage (36). Rnr3 staining is not expected in WT cells in the absence of DNA-damage. The weak basal staining we see in WT cells is comparable to that in a Δrnr3 strain (Supplementary Figure S3). However, with DNA-damage there is a clear induction of Rnr3 expression in WT cells. The Rnr4 antibody worked well in assays where the cells are processed for flow cytometry, and showed proper nuclear localization in the absence of damage. A detergent permeabilization is used in this case. However, in FISH experiments the permeabilization is in 70% ethanol, which can potentially affect the recognition of a protein by its antibody. In our experiments the nuclear to cytoplasmic contrast of Rnr4 was poor when we attempted the simultaneous detection of *RNR4* mRNA and Rnr4 protein. An induction of the signal could still be detected. But because of the lack of proper nuclear localization of Rnr4 in untreated cells, we have left this result out.

Antibody stains for flow cytometry. Cells were grown and spheroplasted as before (except without VRC), permeabilized in 0.2% Tween-20 in Buffer B for 10 minutes, and blocked with 1% BSA in PBS for 1 hr. Antibody stains were then performed as above. Flow cytometry was performed on an Accuri C6 Flow Cytometer.

Image and Statistical analyses. Images were acquired on an Observer Z1 microscope (Carl Zeiss, Jena, Germany) with a Hamamatsu Orca-ER camera (Hamamatsu, Hamamatsu City, Japan). Z-stack images in all channels were obtained. For mRNA spot counting we used an algorithm developed in a previous work (28). This has been used to count mRNA numbers in yeast (37), and we too verified that this works in our case (Supplementary Figure S4). mRNA numbers were reproducible among different experiments, and the variation of the means did not reflect the large variation within the population (Supplementary Figure S5). For evaluating total protein intensity, the edge-detection was performed on the phase image to extract the cell contours, and the antibody stain intensity was evaluated within this mask. The cells have

intrinsic autofluorescence, though this is low in the far-red wavelengths used. The mounting medium also introduces a certain amount of background fluorescence. The effects of these two factors are subtracted out by estimating the mean fluorescence levels in similarly mounted effectively unstained samples treated with just the secondary antibody. This mean intensity is subtracted from the measured intensities. Effort was made to use isolated single cells in all cases. Representative images were processed with ImageJ while all image analysis was performed in Matlab (Mathworks, Natick, MA). Statistical tests and graph plots were performed with Matlab and OriginPro 8.5 (OriginLab, Northampton, MA).

RESULTS

We first used single mRNA molecule FISH to measure *RNR* transcripts in a cell-cycle specific manner. Cell-cycle stage was deduced from nucleus and cell images (Figure 2 and Supplementary Figure S6). In control undamaged cells we found a stark absence of *RNR1* mRNA in nearly all budded cells, i.e. cells in S or G2, and only a subset of control unbudded G1 cells had large amounts of *RNR1* mRNA (Figure 2, Supplementary Figure S7). These results are consistent with previous bulk northern blot studies showing large fluctuations of *RNR1* mRNA in the course of the normal cell-cycle with transcript levels peaking in the late G1/early S phases(15), but the near total absence of *RNR1* mRNA in budded cells was surprising. This indicates that *RNR1* mRNA numbers drop precipitously as cells initiate DNA synthesis. Also consistent with bulk studies (13, 15, 19), *RNR3* mRNA was entirely absent throughout the cell-cycle in undamaged log-phase cells and the cell-cycle dependent differences *RNR2* and *RNR4* transcript numbers were relatively small, though significant for *RNR4* (Figure 2B).

In contrast, cells damaged with the alkylating agent MMS for 1 hour exhibited clear induction of all four *RNR* mRNAs. *RNR1* mRNA was highly induced from near absence in S/G2 cells, and for all *RNR* genes cell-cycle-dependent differences in mRNA numbers that were negligible in control cells became pronounced upon damage (Figure 2B). Thus, overall *RNR* transcriptional inductions observed upon DNA-damage in bulk studies are not mere amplifications of relative distributions of mRNA numbers across the cell-cycle in control untreated cells. Remarkably, G1 mRNA numbers were largely comparable between control and damaged cells for all three normal cell-cycle *RNR* genes (*RNR1*, *RNR2*, *RNR4*), whereas S/G2 numbers were significantly different (Figure 2C). This was unexpected as in previous work, under conditions of DNA damage, cells exhibited induction of *RNR1*, *RNR2* and *RNR3* mRNA in α-factor arrested G1

188 cells with northern blot measurements (14, 15), leading to the conclusion that *RNR* gene
189 induction is independent of the cell-cycle. And while a clear induction was seen, it should be
190 noted that even in these studies the induction of *RNR2* and *RNR3* was lower in α-factor
191 arrested cells compared to asynchronous cells. We investigated this discrepancy by using the
192 same *S. cerevisiae* strain and conditions used in the previous studies, and found that the
193 perceived induction was likely due to a small subpopulation of budded S/G2 cells that escape
194 arrest; this subpopulation had an overwhelming *RNR* response to DNA-damage greatly biasing
195 the mean (Supplementary Figure S8). Importantly 'shmooed' G1 cells showed no significant
196 *RNR2* induction. Also it is possible that α-factor arrested cells activate DNA-damage
197 checkpoints differently from G1 cells in asynchronous cultures. This underscores the importance
198 of studying cells in a normal asynchronous cycling population versus under α-factor arrest, and
199 also the importance of single-cell response studies as opposed to bulk cell responses. Cell-
200 cycle dependent responses in the previous studies were performed with alkylation damage by
201 MMS, though other forms of genotoxic stress were also shown to induce *RNR* expression. It can
202 be expected that the *RNR* response in the cell-cycle would be different for other forms of lesions
203 like double-strand breaks (DSBs) or those caused by ultraviolet (UV) radiation. We tested this
204 possibility for damage by the UV-mimetic agent 4-NQO and the radio-mimetic DSB causing
205 agent bleomycin in terms of the transcriptional responses of the large-subunit (R1) gene *RNR1*
206 and the small-subunit (R2) gene *RNR2*. For both these agents we found that the transcriptional
207 induction response was much larger in S/G2 cells than G1 cells. The induction of *RNR2* in G1
208 was significant, but still much smaller than that in S/G2 cells (Supplementary Figure S9). Thus
209 the cell-cycle dependent induction of *RNR* genes seems to be a general feature of at least three
210 different forms of genotoxic stress. *RNR* induction when present is severely abrogated in G1
211 cells in asynchronous cultures.
212
213 Next, we determined whether the protein induction correlates with transcript induction, and how
214 transcript induction relates to protein localization. We detected endogenous *RNR* mRNA and
215 Rnr protein in the same cells by FISH and antibody staining respectively. Rnr protein levels
216 showed significant induction in S/G2 cells upon damage (Figure 3A). By staining mRNA in the
217 same cells we were able to correlate *RNR1*, *RNR2* and *RNR3* gene products on a cell-by-cell
218 basis (Figure 3B). Fluctuations in mRNA in the normal cell-cycle may not reflect in protein
219 levels. But under conditions of stress, cell-cycle dependent induction of both transcript and
220 protein were observed. Whereas levels were heterogeneous across individual cells, clear
221 induction of mean-levels over cells was seen for both mRNA and protein. Unfortunately the

Rnr4 antibody did not work in the assay for simultaneous detection of mRNA and protein, and this is discussed in the Materials and Methods section.

In addition to R1 (Rnr1 and Rnr3) levels, active RNR enzyme numbers are regulated by the nuclear to cytoplasmic translocation of the R2 proteins (Rnr2 and Rnr4) upon DNA-damage (19, 36) (Figure 1) and Sml1-mediated inhibition of the RNR enzyme (39, 41). There was no obvious relation between Nuclear to Cytoplasmic Ratio (NCR) of Rnr2 and the number of *RNR2* transcripts in control cells. But after one-hour of DNA-damage we observed that the cells that still had nuclear Rnr2 were typically in G1, and that these cells had low *RNR2* transcripts. In contrast S/G2 cells exhibited clearly homogeneous or cytosolic Rnr2 and high numbers of *RNR2* transcripts (Figure 4). While it is known that the Mec1-Rad53 pathway controls both the transcriptional induction of the *RNR* genes (20, 35) and the subcellular relocalization of Rnr2-Rnr4 (23), we show here that both of these responses are cell-cycle-dependent in asynchronous cell populations. In previous studies no nuclear to cytoplasmic translocation of Rnr2 or Rnr4 was observed in α-factor arrested G1 cells, and this was attributed to a possible lower activation of the Mec1-Rad53 pathway in these cells (36). However, recent research has demonstrated that the Mec1 kinase can be activated throughout the cell-cycle by two independent mechanisms dependent on the 9-1-1 complex and DNA polymerase ε (27). This study used the DNA-damage-dependent phosphorylation of the yeast histone H2A at Serine 129 (H2A-S129p) as a direct readout of Mec1 kinase activity (27). Hence we next adapted our approach of simultaneous detection of protein and mRNA to determine whether Mec1 kinase activity varies in the cell-cycle in a manner similar to the *RNR* transcriptional response.

Both asynchronous and α-factor arrested cells showed similar relative inductions H2A-S129p upon DNA-damage in terms of the mean response (Supplementary Figure S10). When we performed simultaneous detection of *RNR2* mRNA and H2A-S129p in the same cells in an asynchronous population, we found an expected correlation between Mec1 kinase activity and *RNR2* induction upon DNA-damage (Figure 5). However, both responses were cell-cycle dependent, and S/G2 cells clearly separated from G1 cells upon damage. The means show similar trends for both *RNR2* and H2A-S129p induction, the few G1 cells that showed high H2A-S129p staining also generally had higher *RNR2* mRNA. Thus, in response to MMS-damage G1 cells display much lower Mec1 kinase activity compared to S/G2 cells. While lower *RNR2* expression in G1 cells was expected, the corresponding lower Mec1 kinase activity was somewhat surprising because a previous study has shown that Mec1 can be activated

throughout the cell-cycle (27), and we too detected Mec1 activity in α-factor arrested cells (Supplementary Figure S10). Future work will explore if this is a peculiarity of the damage caused by MMS, or if the 9-1-1 dependent pathway operating in G1 is less efficient at activating Mec1 than the Pol ε dependent pathway which operates in the S-phase in conjunction to 9-1-1 (27).

Finally, a core strength of investigating single-cell responses is that forms of the underlying distributions across cell populations can be assessed in addition to the means. The *RNR2* mRNA distributions appeared bi-modal when cell cycle stage was ignored, but the two peaks resolved into two overlapping uni-modal distributions when cells were classified according to cell cycle. The two peaks were not as well-resolved in the *RNR4* data. Single-cell level variability or 'noise' in *RNR* mRNA expression generally increased upon DNA damage, with the large subunits exhibiting greater variability in comparison with the small subunits (Figure 6) when resolved according to the cell-cycle stage. Fano factors (σ^2/μ - variance by mean of the distributions) quantify this noise, and a Poissonian distribution has a Fano factor of 1 as expected for mRNA production with constant probability in time (29, 32). 'Transcriptional bursting' can however result in larger variability within the population and consequently higher Fano factors (29). Control, untreated mRNA distributions for all RNRs exhibited Fano factors greater than 1, indicative of noisy, non-Poissonian transcriptional processes (29, 32). While expression noise generally increased upon induction by DNA damage for most of the *RNR*s when parsed according to the cell-cycle, the assumption of a steady-state that is required to mechanistically interpret these distributions is not satisfied due to the transient nature of the DNA-damage response. Similar Fano factors cannot be calculated for the protein distributions as absolute numbers are not measured (29), but these exhibit different forms from the mRNA distributions (Supplementary Figure S11).

DISCUSSION

The principal conclusion of this work is that the *RNR* response to DNA damage does not operate similarly across the cell cycle at either the transcript or the protein level. We also show that these responses correlate even at the single-cell level with each other and with Mec1 kinase activity across the cell-cycle. Control of Rnr protein level and localization in turn regulates RNR enzyme numbers and implies that the dNTP synthesis potential of cell subpopulations varies according to cell-cycle stage under conditions of genotoxic stress. Such

fine-tuning of dNTP levels may possibly minimize spontaneous mutations within the population. Our results concur with a previous study showing that dNTP levels are low in G1 and high in S phase, and that constitutively high dNTP levels transiently arrest cells in late G1 and inhibit the DNA-damage checkpoint (11). It is not well understood why dNTP levels should necessarily be low in G1. Lesion bypass by DNA polymerases has been shown to be dependent on dNTP concentrations (30). In an *in vitro* assay, the replicative DNA polymerase ε could not bypass 4-NQO induced 8-oxoG lesions at normal S-phase concentrations of dNTP, but could bypass it when the concentrations were comparable to the DNA-damage induced state (30). Another independent line of evidence has demonstrated abundant incorporation of ribonucleotides into DNA by yeast replicative polymerases that if left unrepaired can block Pol ε (24). This in turn may activate the Mec1-Rad53 pathway (27) and the downstream *RNR* transcriptional response (20, 35). Given the large molar excess of rNTPs over dNTPs in cells (24), upregulating dNTP production may reduce rNTP misincorporation into DNA. However, it is well known that while dNTPs are essential for responding to genotoxic stress, high dNTP levels are mutagenic and the RNR enzyme is subject to dATP feedback inhibition (10). The Mec1-Rad53-Dun1 target Sml1 too regulates the activity of the RNR enzyme (39, 41).Thus cells have evolved a number of mechanisms for regulating dNTP concentrations by controlling the levels, localization and activation state of the RNR enzyme components. Our work shows that the observed low dNTP levels in G1 can, at least in part, be due to low absolute numbers of the active enzyme in this cell-cycle stage.

Expressions of *RNR2*, *RNR3* and *RNR4* genes are controlled by the transcriptional repressor Crt1, while *RNR1* is under the regulation of the activator Ixr1 through a Dun1 independent branch of the Mec1-Rad53 pathway (20, 35). The resultant highly heterogeneous mRNA distributions are consistent with models of transcriptional bursting of the *RNR* genes (29). Unlike mammalian cells, only a small subset of yeast genes are thought to undergo bursting, and promoter regions in these genes are enriched in TATA elements (38). Only 20% of yeast genes have TATA boxes in their promoters, and these are also enriched in stress related genes (3, 4), which have been shown to exhibit particularly noisy expression (3). The *RNR* genes also have TATA regulatory elements in their promoters (4, 33), supporting the observed non-Poissonian nature of *RNR* transcription under control conditions. Functional consequences of this variability in expression may be important to ensure survival of subpopulations of cells under challenging environmental conditions (1, 29). Future work will explore how the heterogeneity in *RNR* expression promotes cell survival.

In the broader context of gene expression, a previous study that explored simultaneous detection of YFP-tagged *E.coli* proteins and the transcripts that encoded them, found little correlation between the levels of these two gene products (32). However, fluorescent protein signals are severely attenuated in most fixation procedures and both mRNA numbers and protein levels can be affected by the addition of tags. Further, mRNA-protein correlations under conditions of stress have not been explored at the single cell level, as reported here in the model eukaryote *S. cerevisiae*. The methods developed here for monitoring endogenous mRNA and protein levels simultaneously offers important insight into RNR enzyme regulation in eukaryotes, showing clear cell-cycle-dependent partitioning of the *RNR* response both in terms of the mRNA and protein induction, and the subcellular trafficking of Rnr subunits. *RNR* genes are overexpressed in many cancers (7, 8, 21). This work establishes an experimental platform for subsequent studies on the effects of DNA damage in metazoan cells that may serve to investigate the development and progression of cancer, which requires understanding the misregulation of expression patterns at the single-cell level that result in disease phenotype.

ACKNOWLEDGEMENTS

This work was supported by MIT Faculty Start-up Funds, the Samuel A. Goldblith Professorship and an CEHS Pilot Project Grant (deriving from NIH P30-ES002109)(to MB, KT, and AM), NIH R01-CA055042 and DP1-OD006422 (to LDS), and the CSBi Merck-MIT Fellowship (to AM). We thank Professor JoAnne Stubbe for the gift of Rnr antibodies, and for insightful discussions. We thank Professor Narendra Maheshri for insightful discussions, Professor Arjun Raj for initial guidance with the FISH experiments, Professor Katharina Ribbeck for access to the Zeiss Observer Z1 microscope, and Professor Gerald Fink for the gift of the RC634 strain. The fluorophore-labeled DNA oligo probes were purified at the MIT Biopolymers facility.

REFERENCES

1. **Altschuler, S. J., and L. F. Wu.** 2010. Cellular heterogeneity: do differences make a difference? Cell **141:**559-563.
2. **An, X., Z. Zhang, K. Yang, and M. Huang.** 2006. Cotransport of the heterodimeric small subunit of the Saccharomyces cerevisiae ribonucleotide reductase between the nucleus and the cytoplasm. Genetics **173:**63-73.
3. **Bar-Even, A., J. Paulsson, N. Maheshri, M. Carmi, E. O'Shea, Y. Pilpel, and N. Barkai.** 2006. Noise in protein expression scales with natural protein abundance. Nat Genet **38:**636-643.
4. **Basehoar, A. D., S. J. Zanton, and B. F. Pugh.** 2004. Identification and distinct regulation of yeast TATA box-containing genes. Cell **116:**699-709.
5. **Bregman, A., M. Avraham-Kelbert, O. Barkai, L. Duek, A. Guterman, and M. Choder.** 2011. Promoter elements regulate cytoplasmic mRNA decay. Cell **147:**1473-1483.
6. **Cai, L., N. Friedman, and X. S. Xie.** 2006. Stochastic protein expression in individual cells at the single molecule level. Nature **440:**358-362.
7. **Cerqueira, N. M., P. A. Fernandes, and M. J. Ramos.** 2007. Ribonucleotide reductase: a critical enzyme for cancer chemotherapy and antiviral agents. Recent Pat Anticancer Drug Discov **2:**11-29.
8. **Cerqueira, N. M., P. A. Fernandes, and M. J. Ramos.** 2007. Understanding ribonucleotide reductase inactivation by gemcitabine. Chemistry **13:**8507-8515.
9. **Chabes, A., V. Domkin, G. Larsson, A. Liu, A. Graslund, S. Wijmenga, and L. Thelander.** 2000. Yeast ribonucleotide reductase has a heterodimeric iron-radical-containing subunit. Proc Natl Acad Sci U S A **97:**2474-2479.
10. **Chabes, A., B. Georgieva, V. Domkin, X. Zhao, R. Rothstein, and L. Thelander.** 2003. Survival of DNA damage in yeast directly depends on increased dNTP levels allowed by relaxed feedback inhibition of ribonucleotide reductase. Cell **112:**391-401.
11. **Chabes, A., and B. Stillman.** 2007. Constitutively high dNTP concentration inhibits cell cycle progression and the DNA damage checkpoint in yeast Saccharomyces cerevisiae. Proc Natl Acad Sci U S A **104:**1183-1188.
12. **de Godoy, L. M., J. V. Olsen, J. Cox, M. L. Nielsen, N. C. Hubner, F. Frohlich, T. C. Walther, and M. Mann.** 2008. Comprehensive mass-spectrometry-based proteome quantification of haploid versus diploid yeast. Nature **455:**1251-1254.
13. **Domkin, V., L. Thelander, and A. Chabes.** 2002. Yeast DNA damage-inducible Rnr3 has a very low catalytic activity strongly stimulated after the formation of a cross-talking Rnr1/Rnr3 complex. J Biol Chem **277:**18574-18578.
14. **Elledge, S. J., and R. W. Davis.** 1989. DNA damage induction of ribonucleotide reductase. Mol Cell Biol **9:**4932-4940.
15. **Elledge, S. J., and R. W. Davis.** 1990. Two genes differentially regulated in the cell cycle and by DNA-damaging agents encode alternative regulatory subunits of ribonucleotide reductase. Genes Dev **4:**740-751.
16. **Friedberg, E. C., G. C. Walker, W. Siede, R. D. Wood, R. A. Schultz, and T. Ellenberger.** 2006. DNA Repair and Mutagenesis. American Society for Microbiology Press, Washington, D.C.
17. **Gygi, S. P., Y. Rochon, B. R. Franza, and R. Aebersold.** 1999. Correlation between protein and mRNA abundance in yeast. Mol Cell Biol **19:**1720-1730.
18. **Hoeijmakers, J. H.** 2007. Genome maintenance mechanisms are critical for preventing cancer as well as other aging-associated diseases. Mech Ageing Dev **128:**460-462.

19. **Huang, M., and S. J. Elledge.** 1997. Identification of RNR4, encoding a second essential small subunit of ribonucleotide reductase in Saccharomyces cerevisiae. Mol Cell Biol **17:**6105-6113.
20. **Huang, M., Z. Zhou, and S. J. Elledge.** 1998. The DNA replication and damage checkpoint pathways induce transcription by inhibition of the Crt1 repressor. Cell **94:**595-605.
21. **Jordheim, L. P., P. Seve, O. Tredan, and C. Dumontet.** 2011. The ribonucleotide reductase large subunit (RRM1) as a predictive factor in patients with cancer. Lancet Oncol **12:**693-702.
22. **Lee, M. V., S. E. Topper, S. L. Hubler, J. Hose, C. D. Wenger, J. J. Coon, and A. P. Gasch.** 2011. A dynamic model of proteome changes reveals new roles for transcript alteration in yeast. Mol Syst Biol **7:**514.
23. **Lee, Y. D., J. Wang, J. Stubbe, and S. J. Elledge.** 2008. Dif1 is a DNA-damage-regulated facilitator of nuclear import for ribonucleotide reductase. Mol Cell **32:**70-80.
24. **Nick McElhinny, S. A., B. E. Watts, D. Kumar, D. L. Watt, E. B. Lundstrom, P. M. Burgers, E. Johansson, A. Chabes, and T. A. Kunkel.** 2010. Abundant ribonucleotide incorporation into DNA by yeast replicative polymerases. Proc Natl Acad Sci U S A **107:**4949-4954.
25. **Nordlund, P., and P. Reichard.** 2006. Ribonucleotide reductases. Annu Rev Biochem **75:**681-706.
26. **Perlstein, D. L., J. Ge, A. D. Ortigosa, J. H. Robblee, Z. Zhang, M. Huang, and J. Stubbe.** 2005. The active form of the Saccharomyces cerevisiae ribonucleotide reductase small subunit is a heterodimer in vitro and in vivo. Biochemistry **44:**15366-15377.
27. **Puddu, F., G. Piergiovanni, P. Plevani, and M. Muzi-Falconi.** 2011. Sensing of replication stress and Mec1 activation act through two independent pathways involving the 9-1-1 complex and DNA polymerase epsilon. PLoS Genet **7:**e1002022.
28. **Raj, A., P. van den Bogaard, S. A. Rifkin, A. van Oudenaarden, and S. Tyagi.** 2008. Imaging individual mRNA molecules using multiple singly labeled probes. Nat Methods **5:**877-879.
29. **Raj, A., and A. van Oudenaarden.** 2009. Single-molecule approaches to stochastic gene expression. Annu Rev Biophys **38:**255-270.
30. **Sabouri, N., J. Viberg, D. K. Goyal, E. Johansson, and A. Chabes.** 2008. Evidence for lesion bypass by yeast replicative DNA polymerases during DNA damage. Nucleic Acids Res **36:**5660-5667.
31. **Tan, R. Z., and A. van Oudenaarden.** 2010. Transcript counting in single cells reveals dynamics of rDNA transcription. Mol Syst Biol **6:**358.
32. **Taniguchi, Y., P. J. Choi, G. W. Li, H. Chen, M. Babu, J. Hearn, A. Emili, and X. S. Xie.** 2010. Quantifying E. coli proteome and transcriptome with single-molecule sensitivity in single cells. Science **329:**533-538.
33. **Tomar, R. S., S. Zheng, D. Brunke-Reese, H. N. Wolcott, and J. C. Reese.** 2008. Yeast Rap1 contributes to genomic integrity by activating DNA damage repair genes. Embo J **27:**1575-1584.
34. **Trcek, T., D. R. Larson, A. Moldon, C. C. Query, and R. H. Singer.** 2011. Single-molecule mRNA decay measurements reveal promoter- regulated mRNA stability in yeast. Cell **147:**1484-1497.
35. **Tsaponina, O., E. Barsoum, S. U. Astrom, and A. Chabes.** 2011. Ixr1 is required for the expression of the ribonucleotide reductase Rnr1 and maintenance of dNTP pools. PLoS Genet **7:**e1002061.

36. **Yao, R., Z. Zhang, X. An, B. Bucci, D. L. Perlstein, J. Stubbe, and M. Huang.** 2003. Subcellular localization of yeast ribonucleotide reductase regulated by the DNA replication and damage checkpoint pathways. Proc Natl Acad Sci U S A **100:**6628-6633.
37. **Youk, H., A. Raj, and A. van Oudenaarden.** 2010. Imaging single mRNA molecules in yeast. Methods Enzymol **470:**429-446.
38. **Zenklusen, D., D. R. Larson, and R. H. Singer.** 2008. Single-RNA counting reveals alternative modes of gene expression in yeast. Nat Struct Mol Biol **15:**1263-1271.
39. **Zhao, X., A. Chabes, V. Domkin, L. Thelander, and R. Rothstein.** 2001. The ribonucleotide reductase inhibitor Sml1 is a new target of the Mec1/Rad53 kinase cascade during growth and in response to DNA damage. Embo J **20:**3544-3553.
40. **Zhao, X., E. G. Muller, and R. Rothstein.** 1998. A suppressor of two essential checkpoint genes identifies a novel protein that negatively affects dNTP pools. Mol Cell **2:**329-340.
41. **Zhao, X., and R. Rothstein.** 2002. The Dun1 checkpoint kinase phosphorylates and regulates the ribonucleotide reductase inhibitor Sml1. Proc Natl Acad Sci U S A **99:**3746-3751.

FIGURES AND FIGURE LEGENDS

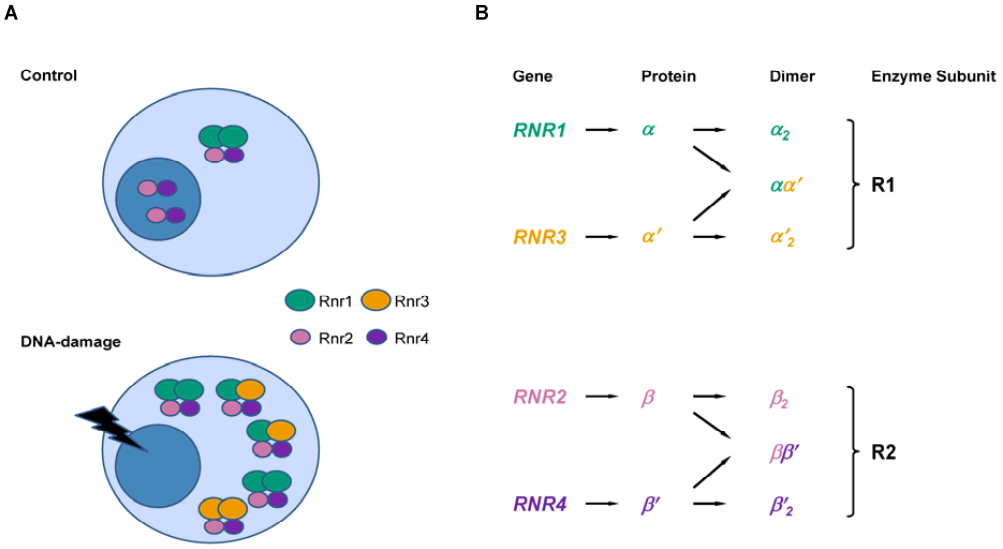

Figure 1. *S. cerevisiae* RNR enzyme response to damage. (A) The functional RNR holoenzyme consists of a large and a small subunit, in almost all eukaryotes from yeast to humans. The form of the enzyme can be more complex than $\alpha_2\beta_2$. Levels of all Rnr proteins go up, and Rnr2-Rnr4 translocate to the cytoplasm upon DNA-damage in *S. cerevisiae*. (B) The cytosolic Rnr1 and Rnr3 proteins constitute the large subunit, R1 and the Rnr2 and Rnr4 proteins constitute the small subunit (R2). The active form of the small subunit is an Rnr2-Rnr4 heterodimer (ββ'), which normally resides in the nucleus but relocalizes to the cytoplasm upon DNA-damage. Rnr3 is not expressed in the absence of DNA-damage.

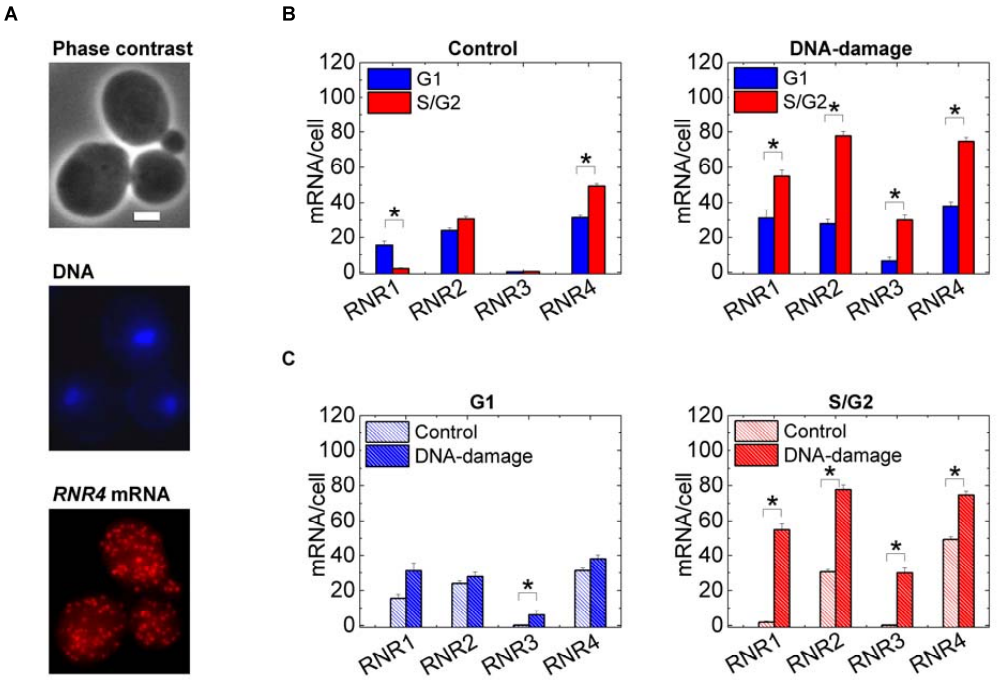

Figure 2. RNR mRNA induction depends on cell-cycle stage. (A) A typical single-molecule mRNA FISH experiment is shown. *RNR4* mRNA transcripts are targeted with Alexa 568-labeled DNA oligo probes. DAPI stained DNA and phase-contrast images are also acquired to judge cell-cycle stage. The scale-bar shown is 2 μm. Z-projected images for the mRNA and DNA are shown. (B) Mean-numbers computed from mRNA distribution histograms for approximately 90-120 such cells are plotted for *RNR1*, *RNR2*, *RNR3* and *RNR4* mRNA for control cells and under conditions of DNA-damage by treatment with 0.02% MMS for 1 hour. Blue bars indicate unbudded G1 cells while red bars denote budded S/G2 cells. While absolute numbers of *RNR1* mRNA is lower than *RNR2* and *RNR4* in untreated cells, the relative fluctuation is greatest for *RNR1* due to the near-complete absence in budded cells (see also Figure 6 for *RNR1* mRNA distributions). The relative distributions shift unexpectedly upon DNA-damage. (C) The same data as (B) parsed according to the cell-cycle stage to compare mRNA numbers in one cell-cycle stage between control and damaged cells. Light-hatched bars denote control cells while dense-hatched bars denote damaged cells. In all cases the error-bars are standard errors. '*' indicates $p<10^{-3}$ in a Kolmogorov-Smirnov test (a non-parametric test is preferable given the non-normal nature of some of the mRNA distributions).

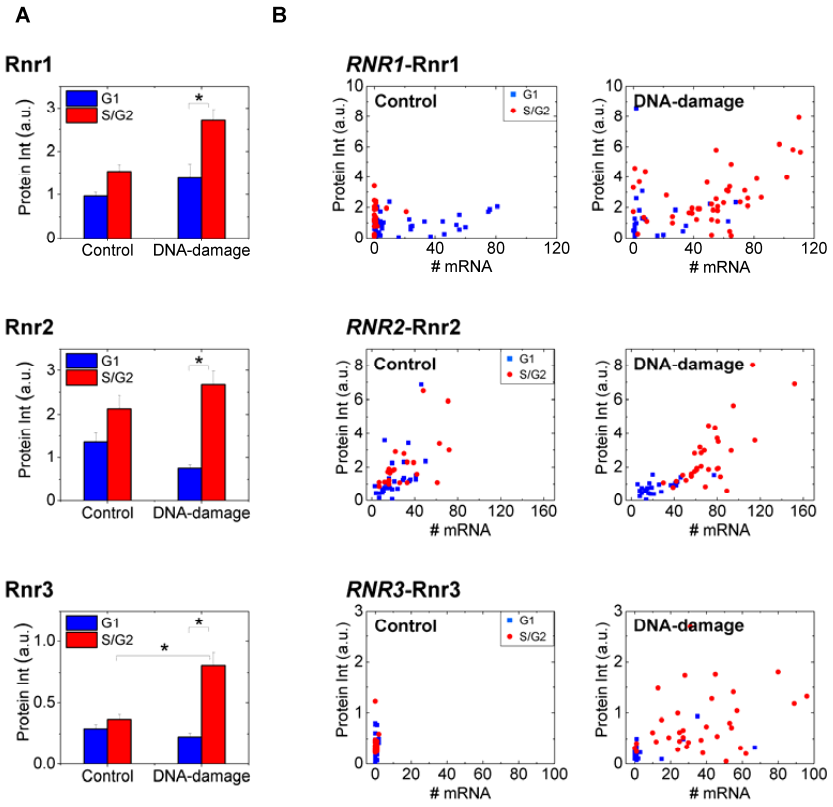

Figure 3. *RNR* transcript numbers show a cell-cycle dependent relation to protein levels and localization upon DNA damage. (A) Mean Rnr protein intensities with standard errors and (B) mRNA numbers and protein intensities on a cell-by-cell basis are plotted for Rnr1 (N=71 cells), Rnr2 (N=57 cells) and Rnr3 (N=64 cells). Equal numbers of cells were considered for the control and DNA-damage (1 hr) samples. The staining for Rnr3 in the absence of damage was non-specific. In every graph blue squares or bars indicate G1 cells while red circles or bars indicate S/G2 cells. Note while S/G2 cells have little or no *RNR1* mRNA (like Figure 2) compared to G1 cells, the protein levels are similar in untreated control cells. A clear separation of G1 and S/G2 cells in MMS treated samples was observed. '*' indicates $p<10^{-3}$ in a Kolmogorov-Smirnov test.

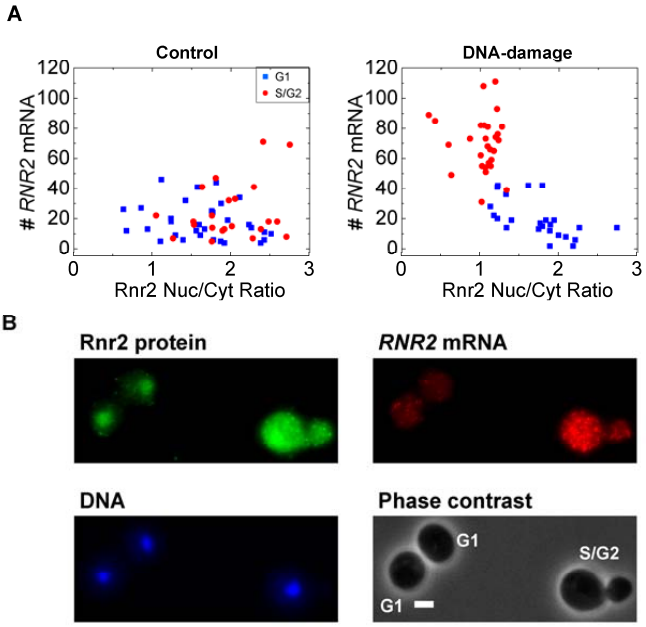

506

507 **Figure 4. *RNR2* transcript numbers show a cell-cycle dependent relation to Rnr2 protein**
508 **localization upon DNA damage.** (A) In the control population *RNR2* mRNA number in cells are
509 uncorrelated with the nuclear to cytoplasmic ratio of Rnr2 and there is no obvious segregation in
510 the cell-cycle. However, upon DNA-damage the S/G2 cells show a higher accumulation of Rnr2
511 in the cytoplasm and higher induction of *RNR2* mRNA (N=53 cells each). (B) A typical image is
512 shown for the small-subunit Rnr2 upon DNA-damage. Rnr2 is normally nuclear-localized in
513 control cells. At the one-hour time-point there are still cells with nuclear Rnr2. The G1 cells with
514 nuclear Rnr2 have fewer *RNR2* transcripts, while the S/G2 cell shows visibly larger *RNR2*
515 expression and a homogenous distribution of the Rnr2 protein. The scale-bar shown is 2 μm. Z-
516 projected images for the DNA, mRNA and protein are shown. The cell-cycle stages are
517 indicated.

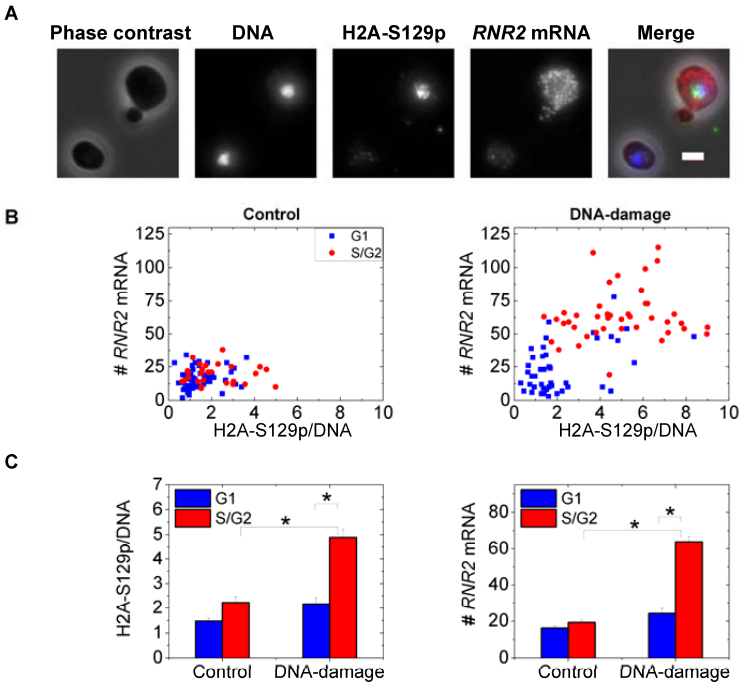

Figure 5. *RNR2* induction correlates with variable Mec1 kinase activity in the cell-cycle. (A) Two typical cells from an MMS-treated sample are shown. Note the higher H2A-S129p staining, indicative of Mec1 kinase activity, in the budded cell correlates with higher *RNR2* mRNA numbers. The scale-bar shown is 2 μm. In the merged image, DNA is in blue, H2A-S129p in green, *RNR2* mRNA in red and the phase image is grey. (B) *RNR2* mRNA numbers are plotted against H2A-S129p stain intensity in control untreated cells and MMS-treated cells (N=85 cells each). The Pearson's r value for the untreated sample is 0.16 while it is 0.6 with DNA-damage. The H2A-S129p stain intensity is normalized by the DNA-intensity evaluated in the same nuclear mask to ensure that the differential response between G1 and S/G2 cells is not merely a function of DNA synthesis. (C) The mean values for the H2A-S129p stain intensity and *RNR2* mRNA from the graphs in (B). '*' indicates $p<10^{-3}$ in a Kolmogorov-Smirnov test.

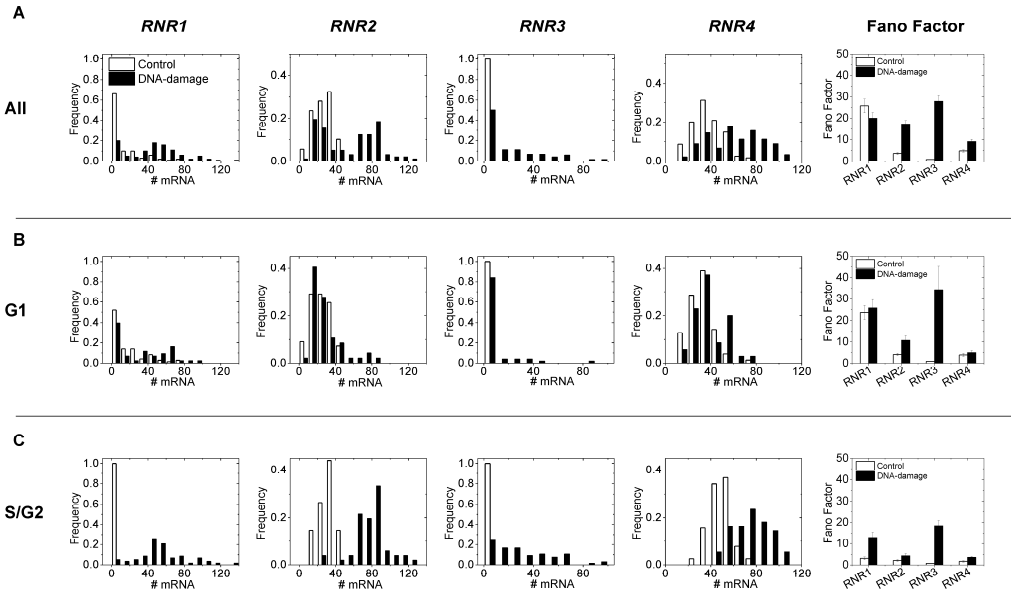

Figure 6. mRNA histograms capture heterogeneity within the cell population. mRNA histograms and corresponding Fano factors for the studied RNR genes for (A) all cells (B) G1 cells (C) S/G2 cells. White bars denote control cells while black bars denote damaged cells. When expressed all RNR genes have Fano factors greater than 1, indicating non-Poissonian transcription processes. Note the higher Fano factors for damaged cells generally when parsed according to the cell-cycle, though this is within error-bars for *RNR1* in G1. Also when they are expressed, R1 genes have higher Fano factors than R2 genes. The error-bars of the Fano factors are standard deviations obtained by bootstrapping from the distributions on the left.